

NASA Technical Memorandum 83708
AIAA-84-1379

On Modeling Dilution Jet Flowfields

J. D. Holdeman
Lewis Research Center
Cleveland, Ohio

and

R. Srinivasan
The Garrett Turbine Engine Company
Phoenix, Arizona 85010

Prepared for the
Twentieth Joint propulsion Conference
cosponsored by the AIAA, SAE, and ASME
Cincinnati, Ohio June 11-13, 1984

NASA

ON MODELING DILUTION JET FLOWFIELDS

by J. D. Holdeman*

NASA Lewis Research Center
Cleveland, OH 44135

and

R. Srinivasan**

The Garrett Turbine Engine Company
Phoenix, AZ 85010

Abstract

This paper compares temperature field measurements from selected experiments on a single row, and opposed rows, of jets injected into a ducted crossflow with profiles calculated using an empirical model based on assumed vertical profile similarity and superposition, and distributions calculated with a 3-D elliptic code using a standard K-E turbulence model. The empirical model predictions are very good within the range of the generating experiments, and the numerical model results, although exhibiting too little mixing, correctly describe the effects of the principal flow and geometric variables.

Introduction

The problem of jets-in-crossflow has been rather extensively treated in the literature, to the point that it can almost be called a "classical" three-dimensional flow problem. Although these studies, of chimney plumes, exhaust from V/STOL aircraft, discharges into rivers and streams, film cooling, and hot gas dilution etc., have all contributed additional understanding of the general problem, the information obtained in any given study is determined by its motivating application, and may not satisfy the specific needs of other diverse problems.

One factor making the combustor dilution zone jet-in-crossflow application unique is that it is a confined mixing problem, with from 10 to 50 percent of the total flow entering through the dilution jets. The result is that the equilibrium temperature

of the exiting flow may differ significantly from that of the entering mainstream flow. To control or tailor the combustor exit temperature pattern it is necessary to be able to characterize the exit distribution in terms of the upstream flow and geometric variables. This requires that the entire flow field be either known or modeled.

Considerations of dilution zone mixing in gas turbine combustion chambers have motivated several studies of the mixing characteristics of single and multiple jets injected into a crossflow in a constant area duct.¹⁻⁹ Recently, experimental results have been reported which provide insight into the effect of several geometric and flow variations characteristic of most gas turbine combustion chambers, namely a variable temperature mainstream, flow area convergence, and opposed rows of jets, either in-line or staggered.¹⁰⁻¹⁴

From the data of references 1, 11, and 14, an empirical model was developed^{4,5} and extended^{11,14} for predicting the temperature field downstream of a single row, or opposed rows, of jets mixing with a confined crossflow. An interactive microcomputer program (Apple DOS 3.3) based on the model of reference 5 was used in reference 9 to study the effects of separately varying the momentum flux ratio, density ratio, orifice size, and orifice spacing, and to identify the relationship among these parameters which optimizes* the mixing.

Although empirical correlation of experimental data can provide an excellent predictive capability within the parameter range of the generating experiments, they must be used with caution, or not at all, outside this range. Physical modeling, in various levels of sophistication and complexity, may be used to obviate this weakness. In this regard, several one and

To be presented as paper AIAA-84-1379 at the AIAA/SAE/ASME 20th Joint Propulsion Conference, Cincinnati, Ohio, June 11-13, 1984.

* Aerospace Engineer, Combustion Branch. Member AIAA

** Engineering Specialist, Aerothermal Component Design.

This paper is declared a work of the U. S. Government and therefore is in the public domain.

+ Although it is recognized that a uniform temperature distribution may not always be desired, "optimum" is used here, as in refs. 2, 5, 9, & 13, to identify geometries which, for a given flow condition, result in a uniform temperature distribution in a minimum downstream distance.

two dimensional integral and differential jet-in-crossflow models are extant which have been shown to give, for example, trajectory predictions that are in good agreement with experiments. These models may provide insight into the dominant physical mechanism(s), and predict some of the characteristic parameters well, but they rarely provide sufficient information to quantify all of the important flow field variables (e.g. temperature, pressure, velocity, and turbulence quantities) in three coordinate directions.

Recently, rapid advances have been made in the capability of computational fluid dynamics models and their application to complex flows such as jet(s)-in-crossflow.¹⁵⁻¹⁸ These models are, however, still in the development and verification stage. They have been shown to be capable of predicting trends in complex flows, but their capability to provide accurate, quantitative and grid independent calculations of these flows has not yet been demonstrated.

The present paper will compare temperature field measurements from selected cases in references 11 and 14 with distributions calculated using an empirical model based on assumed vertical profile similarity and superposition,^{11, 14} and a 3-D elliptic code with a standard K-E turbulence model.¹⁷ The results will show the capability (or lack thereof) of the models to predict the effects of the principal flow and geometric variables.

Description of Models

The empirical model for the temperature field downstream of jets mixing with a confined crossflow is based on the observation that properly non-dimensionalized vertical temperature profiles everywhere in the flow field can be expressed in the following self-similar form⁵

$$\frac{(T_{max}^{+/-} - T)}{(T_{max}^{+/-} - T_c)} = \frac{-(\ln 2)(y - y_c)^2}{\exp(W_{1/2}^{+/-})^2} \quad (1)$$

where T is the temperature at vertical location y, and T_{max}^{+/-}, W_{1/2}^{+/-}, T_c, and y_c are scaling parameters (see Nomenclature). Correlations have been developed for each of these in terms of the independent variables J, S/D, H₀/D, Z/S, and X/H₀. The correlation of reference 5 for a single row of jets in a uniform temperature crossflow have been extended for predicting the temperature field downstream of single or opposed rows of jets, either in-line or staggered, injected into an isothermal or non-isothermal mainstream, with and without

flow area convergence.^{11, 14} A major weakness of these (and previous) correlations is that their form precludes their use for semi confined flows (large H₀/D or S/D), single jet flows, or flows in which it is known a priori that the primary assumptions in the model will be violated.

Numerical models do not have these limitations, and in addition provide calculations for all flow quantities of interest, not just those which happen to have been empirically correlated. The code used in this investigation is based on the USARTL 3-D model,¹⁹ and uses pressure and velocities as the main hydrodynamic variables. This code, or similar versions thereof, has been used in previous validation and assessment studies.¹⁵⁻¹⁸

The governing equations are represented by finite difference approximations on a staggered grid system. The differencing technique employed is hybrid for convective terms with central differencing of all other terms. The velocity-pressure coupling is handled by the SIMPLE algorithm of Patankar and Spalding.^{20, 21} Uniform velocities, and mass flow rates were used at all in-flow boundaries. The turbulent Schmidt Number was 0.9, the RMS turbulence intensity was chosen to be 5.5 percent of the local mean velocity, and the inlet length scale was 2 percent of the jet diameter and duct height for the jet and mainstream respectively. Standard values of the turbulence constants were used in all calculations.

Numerous uncertainties are currently present in 3-D calculations due to, for example, numerical diffusion, unmeasured (and hence assumed) boundary conditions, and turbulence model assumptions. The results shown here are not intended to represent the "best" agreement possible from numerical models at this time, as better temperature field agreement could undoubtedly have been achieved by adjusting model constants and/or inlet boundary conditions. Since this was not necessary to satisfy the present objective of evaluating the potential of these codes vis-a-vis combustor dilution zone flowfields, and due to the substantial uncertainties in the numerical calculation and because the mean temperature was the only parameter compared, no adjustments were made.

Results and Discussion

Figure 1 shows a schematic of the dilution jet flowfield of interest in this paper. The temperature field results are presented in three-dimensional oblique views of the temperature difference ratio, THETA, where

$$THETA = \frac{(T_m - T)}{(T_m - T_j)} \quad (2)$$

Note that THETA = 1 if the local temperature is equal to the jet

temperature, and $\theta = 0$ if the local temperature is equal to the mainstream temperature. The equilibrium θ for any configuration is equal to the fraction of the total flow entering through the dilution jets, W_j/W_T .

In the 3-D plots the temperature distribution is shown in planes normal to the main flow direction. The coordinates y and z are, respectively, normal to and along the orifice row in this constant x plane. The orifice configurations investigated are shown in figure 2. For clarity and consistency of the visual presentation, the θ distributions are shown over a 2S span in the z -direction, with the plane between jets, the midplane, at the edge of the oblique plots.

The following paragraphs, and the 3-D plots in figures 3 to 11, compare the experimental data with the empirical and numerical model results, in the context of the effects of the primary independent variables. The flow and geometry conditions corresponding to these figures are given in table 1. Isotherm contour plots and centerplane temperature profile plots for these conditions are given in reference 22.

Variations with Orifice Size and Spacing. At constant orifice area, changes in orifice size and spacing can have a significant influence on the θ profiles. This is shown in parts a) and b) of both figures 3 and 4, where jets from closely spaced small orifices under-penetrates and remain near the injection wall, and jets from widely spaced larger orifices over-penetrates and impinge on the opposite wall.

The empirical model reproduces the data very well in the small orifice case, since the data are consistent with the major assumption in the empirical model, that all vertical temperature distributions can be reduced to similar Gaussian profiles. The empirical model does not do as well in the larger orifice case however, as the impingement of the jets on the opposite wall results in vertical profiles which are not similar.

The numerical model calculations made with approximately 20,000 nodes, although in qualitative agreement with the data, show temperature gradients that are too steep, especially in the transverse direction. Under-prediction of the mixing was seen in the single-jet calculations of reference 15 also, where it is shown that the isotropic turbulence model under-estimates the intensity. The result in figures 3 and 4 is typical of the numerical model calculations to be shown in this paper.

For the small-orifice case a coarse-grid calculation using less than 6000 nodes was also performed. The numerical results in figures 3a) and 4a) illustrate the significant influence of grid selection on the solution obtained, and the smearing of

the profiles which can occur as a result of numerical diffusion.

Coupled Spacing and Momentum Flux Ratio. Examination of the experimental data revealed that similar jet penetration is obtained over a range of momentum flux ratios, independent of orifice diameter, if orifice spacing and momentum flux ratio are correctly coupled.^{2,5,7,13} For example, low momentum flux ratios require large, widely spaced holes, whereas smaller closely spaced holes are appropriate for high momentum flux ratios, as shown in figures 5 and 6.

In general, jet penetration and centerplane profiles are similar when the spacing is inversely proportional to the square root of the momentum flux ratio, i.e.:

$$S/H_o = C / (\text{SQRT}(J)) \quad (3)$$

For single-side injection, the centerplane profiles are approximately centered across the duct height and approach an isothermal distribution in the minimum downstream distance when $C=2.5$. This appears to be independent of orifice diameter, as shown in both the calculated and experimental profiles in figures 7 and 8.

Values of C in equation (3) which are a factor of ≥ 2 smaller or larger than the optimum correspond to under-penetration or over-penetration respectively (e.g. figures 3 and 4).

In all of the combinations shown in figures 5, 6, 7, and 8 the empirical model results are in very good agreement with the data, as the data are consistent with the Gaussian profile assumption. The numerical model calculations using approximately 20,000 nodes for these cases show jet penetration which is in good agreement with the data, but the mixing is otherwise under-predicted as described previously.

Examination of the empirical model results in figures 3 to 8 in the context of equation (3) suggests that in general the empirical model would be expected to provide good temperature field predictions for single-side injection when $1 < (S/H_o)(\text{SQRT}(J)) < 5$. It is significant to note that the numerical model is not subject to this inherent limitation.

Variable Temperature Mainstream. The influence of a non-isothermal mainstream flow on the profiles for medium momentum flux ratios with $S/H_o=.5$ and $H_o/D=4$ can be seen by comparing figure 9 with figures 7b) and 8b). The shape of the experimental profiles in figure 9 suggests modeling them as a superposition of the upstream profile and the corresponding jets-in-an-isothermal mainstream distribution.¹³ The hottest temperature in the mainstream flow was used as T_m in the definition

of THETA (see equation (2)) for this case.

This gives a good approximation, as seen in the empirical model results. The agreement is only first-order however, since with a variable temperature mainstream there can be cross-stream thermal transport due to the flow of mainstream fluid around the jets (and hence to different y locations), and this is not accounted for in superimposing the distributions. This becomes apparent if the local mainstream temperature, $T_m(x,y)$, is used in the definition of THETA in equation (2).

In the variable temperature mainstream case the numerical model results agree well with the experimental data, especially on the jet centerplane, but the transverse mixing is underpredicted, as in the corresponding isothermal mainstream case in part b) of figures 7 and 8.

Opposed Rows of In-line Jets. For opposed rows of jets, with the orifice centerlines in-line, the optimum ratio of orifice spacing to duct height is one-half of the optimum value for single-side injection at the same momentum flux ratio.¹³ As an example consider the single-side case with $S/H_o=0.5$ and $H_o/D=4$ in figures 7b) and 8b), and the opposed row of in-line jets with $S/H_o=0.25$ and $H_o/D=8$ in figure 10. Note that the product of the spacing and the square root of the momentum flux ratio (C in equation (3)) is 1.25 for this case, or one-half of the optimum value for single-side injection.

The empirical model predicts the opposed-jet case very well, verifying the primary assumption that the effect of a plane of symmetry is similar to that of an opposite wall.^{3,9,13} Note that the experimental profiles on both sides of the plane of symmetry support the Gaussian profile assumption. The numerical model results show the steep transverse and lateral gradients indicative of too little mixing, as seen in almost all of the previous calculations also, but the penetration and profile shape are in good agreement with the data.

Opposed Rows of Staggered Jets. For opposed rows of jets, with the orifice centerlines staggered, the optimum ratio of orifice spacing to duct height is double the optimum value for single-side injection at the same momentum flux ratio.¹³ As an example consider the single-side case with $S/H_o=0.5$ in figures 7b) and 8b) ($C = (S/H_o)(\text{SQRT}(J)) = 2.16$), and the opposed row of staggered jets with $S/H_o=1$ in figure 11 ($C = 5.25$).

The empirical model does not handle this complex case well, as the fluid dynamic interactions here are not amenable to a direct extension of the simple Gaussian profile and superposition type modeling appropriate for most of the single-side and

opposed-jet cases of interest. The numerical model calculations, are not in appreciably better agreement with the data than the empirical model results, as the mixing is under-predicted here as in the previous cases.

As in most of the previous numerical calculations, approximately 20,000 grid points were used, but note that twice as many grid nodes were required in the transverse direction in this case, and that the number of axial grid points was correspondingly reduced. The number of axial nodes used in this calculation is approximately the same as that used in the coarse grid calculations shown in figures 3a), 4a), 5b), and 6b). It follows that the numerical diffusion in the x -direction would be comparable between these calculations.

The numerical result for the staggered jet case is encouraging in that this method is not restricted by profile assumptions as is the empirical model, and the numerical model results should improve with overall improvements in the capability of the 3-D codes.

Summary of Results

The present paper compares temperature field measurements from selected experiments, wherein a single row, or opposed rows, of jets were injected into a ducted crossflow, with distributions calculated with an empirical model based on assumed vertical profile similarity and superposition and with a 3-D elliptic code using a standard K-E turbulence model. The empirical model calculations of the temperature field are very good within the parameter range of the generating experiments whenever the primary assumptions in the model are supported by the experimental data.

Although the numerical model calculations consistently exhibit too little mixing, the trends which result from variation of the independent flow and geometric variables are approximated correctly. Codes with improved numerics, accuracy, and turbulence models should provide more quantitative predictions. Of note is the fact that the 3-D codes can provide calculations for complex flows that are outside the range of available experiments, or for which the assumptions in the empirical model are known a priori, to be invalid. Also important is the fact that the 3-D codes provide a prediction for all flowfield quantities (i.e. velocity, turbulence, etc.), not just those that have been empirically modeled.

References

1. Walker, R.E. and Kors, D.L., "Multiple Jet Study Final Report," NASA CR-121217, June 1973.
2. Holdeman, J.D., Walker, R.E., and Kors, D.L., "Mixing of Multiple Dilution Jets with a Hot Primary Airstream for Gas Turbine Combustors," AIAA Paper 73-1249, Nov. 1973 (NASA TM X-71426).
3. Kamotani, Y. and Greber, I., "Experiments on Confined Turbulent Jets in Cross Flow," NASA CR-2392, Mar. 1974.
4. Walker, R.E. and Eberhardt, R.G.: Multiple Jet Study Data Correlations. NASA CR-134795, April 1975.
5. Holdeman, J.D. and Walker, R.E., "Mixing of a Row of Jets with a Confined Crossflow," *AIAA Journal*, vol.15, no.2, Feb. 1977, pp.243-249 (AIAA Paper 76-48; NASA TM-71821).
6. Cox, G.B. Jr., "Multiple Jet Correlations for Gas Turbine Engine Combustor Design," *Journal of Engineering for Power*, Vol. 98, No. 2, 1976, pp.265-273.
7. Cox, G.B. Jr., "An Analytical Model for Predicting Exit Temperature Profile from Gas Turbine Engine Annular Combustors," AIAA Paper 75-1307, Sept. 1975.
8. Khan, Z.A., McGuirk, J.J., and Whitelaw, J.H., "A Row of Jets in Crossflow," *Fluid Dynamics of Jets with Application to U/SIOL*, AGARD-CP-308, Technical Editing and Reproduction. London, 1982.
9. Holdeman, J.D., "Perspectives on the Mixing of a Row of Jets with a Confined Crossflow," AIAA Paper 83-1200, June 1983 (NASA TM 83457).
10. Atkinson, K.N., Khan, Z.A., and Whitelaw, J.H., "Experimental Investigation of Opposed Jets Discharging Normally into a Cross-stream," *Journal of Fluid Mechanics*, Vol.115, 1982, pp.493-504.
11. Srinivasan, R., Berenfeld, A., and Mongia, H.C., "Dilution Jet Mixing Phase I Report," Garrett Turbine Engine Co., Phoenix, Ariz., Garrett 21-4302, Nov. 1982. (NASA CR-168031).
12. Wittig, S.L.K., Elbahar, O.M.F., and Noll, B.E.: Temperature Profile Development in Turbulent Mixing of Coolant Jets with a Confined Hot Cross-Flow," ASME Paper No. 83-GT-220, Mar. 1983.
13. Holdeman, J.D., and Srinivasan, R., "Experiments in Dilution Jet Mixing." AIAA Paper 83-1201, June 1983. (NASA TM 83457).
14. Srinivasan, R., Coleman, E., Johnson, K., and Mongia, H.C., "Dilution Jet Mixing Program Phase II Report." Garrett 21-4804, December 1983. (NASA CR-174624).
15. Claus, R.W., "Analytical Calculation of a Single Jet in Crossflow and Comparison with Experiment," AIAA Paper 83-0238, January 1983 (NASA TM 83027).
16. Sturgess, Geoffrey J., "Aerothermal Modeling Phase I Final Report," Pratt & Whitney Aircraft, E. Hartford, Conn., PWA-5907-19, May 1983. (NASA CR-168202).
17. Srinivasan, R., Reynolds, R., Ball, I., Berry, R., Johnson, K., and Mongia, H.C., "Aerothermal Modeling Program: Phase I Final Report," Garrett Turbine Engine Co., Phoenix, Ariz., Garrett 21-4742, Aug. 1983 (NASA CR-168243).
18. Kenworthy, M.J., Correa, S.M., and Burrus, D.L., "Aerothermal Modeling Phase I - Final Report," NASA CR-168296, General Electric Company, Cincinnati, Ohio, November 1983.
19. Bruce, T.W., Mongia, H.C., Reynolds, R.S., "Combustor Design Criteria Validation," AiResearch Manufacturing Co. of Arizona, Phoenix, AZ, Report 75-211682(38), March 1979. (USARTL-TR-78-55A, B, and C).
20. Patankar, S.V., and Spalding, D.B., "A Calculation Procedure for Heat, Mass, and Momentum Transfer in Three-Dimensional Parabolic Flows," *International Journal of Heat and Mass Transfer*, Vol.15, No.10, Oct 1972, pp.1787, 1806.
21. Patankar, S., and Spalding, D., "A Computer Model for Three-Dimensional Flow in Furnaces," *14th Symposium (International) on Combustion*, The Combustion Institute, Pittsburgh, 1973, pp.605-614.
22. Holdeman, J.D., and Srinivasan, R., "Modeling of Dilution Jet Flowfields," NASA CP-2309, April 1984, pp.175-187.

Nomenclature

- A_j/A_m = jet-to-mainstream area ratio
= $(\pi/4)/((S/H_o)(H_o/D)^2)$ for one-side injection
= $(\pi/2)/((S/H_o)(H_o/D)^2)$ for two-side injection
- C_d = orifice discharge coefficient
- D = orifice diameter
- D_j = $(D)(\text{SQRT}(C_d))$
- DR = jet-to-mainstream density ratio = (T_m/T_j)
- H_o = duct height
- J = jet-to-mainstream momentum flux ratio = $(DR)(R)^2$
- M = jet-to-mainstream mass flux ratio = $(DR)(R)$
- R = jet-to-mainstream velocity ratio = (V_j/U_m)
- S = spacing between orifice centers
- T = temperature
- T_c = temperature at y_c
- T_j = jet exit temperature
- T_m = mainstream temperature
- $T_{\max}^{+/-}$ = maximum temperature above (+) or below (-) the centerline
= $T_m - (T_m - T_j)(\text{THETA}_{\min}^{+/-})$; see ref.5
- THETA = $(T_m - T)/(T_m - T_j)$
- U = velocity
- U_m = mainstream velocity
- V_j = jet velocity
- w_j/w_T = jet-to-total mass flow ratio
= $\frac{(\text{SQRT}((DR)(J)))(C_d)(A_j/A_m)}{1 + (\text{SQRT}(DR)(J))(C_d)(A_j/A_m)}$
- $w_{1/2}^{+/-}$ = jet half-widths above (+) or below (-) the centerline; see ref.5
- x = downstream coordinate
= 0 at injection plane
- y = cross-stream (radial) coordinate
= 0 at wall
= y_c at location of minimum temperature in a line $x=\text{const}$, $z=\text{const}$
- z = lateral (circumferential) coordinate
= 0 at centerplane

Table 1. Flow and Geometry Conditions

| Figure | S/H ₀ | H ₀ /D | A _j /A _m | C _d | DR | J | W _j /W _T | (S/H ₀) (SQRT(J)) |
|--------|------------------|-------------------|--------------------------------|----------------|-----|------|--------------------------------|-------------------------------|
| 3a, 4a | .25 | 8. | .05 | .60 | 2.1 | 22.4 | .17 | 1.18 |
| 3b, 4b | 1.0 | 4. | .05 | .67 | 2.2 | 23.5 | .19 | 4.85 |
| 5a, 6a | 1.0 | 4. | .05 | .73 | 2.1 | 5.3 | .11 | 2.30 |
| 5b, 6b | .25 | 8. | .05 | .61 | 2.3 | 92.7 | .30 | 2.41 |
| 7a, 7b | .5 | 5.7 | .05 | .71 | 2.2 | 25.4 | .21 | 2.52 |
| 7b, 8b | .5 | 4. | .10 | .61 | 2.1 | 18.6 | .27 | 2.16 |
| 9 | .5 | 4. | .10 | .61 | 1.8 | 31.3 | .31 | 2.80 |
| 10 | .25 | 8. | .10 | .65 | 2.1 | 25.0 | .32 | 1.25 |
| 11 | 1.0 | 4. | .10 | .65 | 2.1 | 27.6 | .33 | 5.25 |

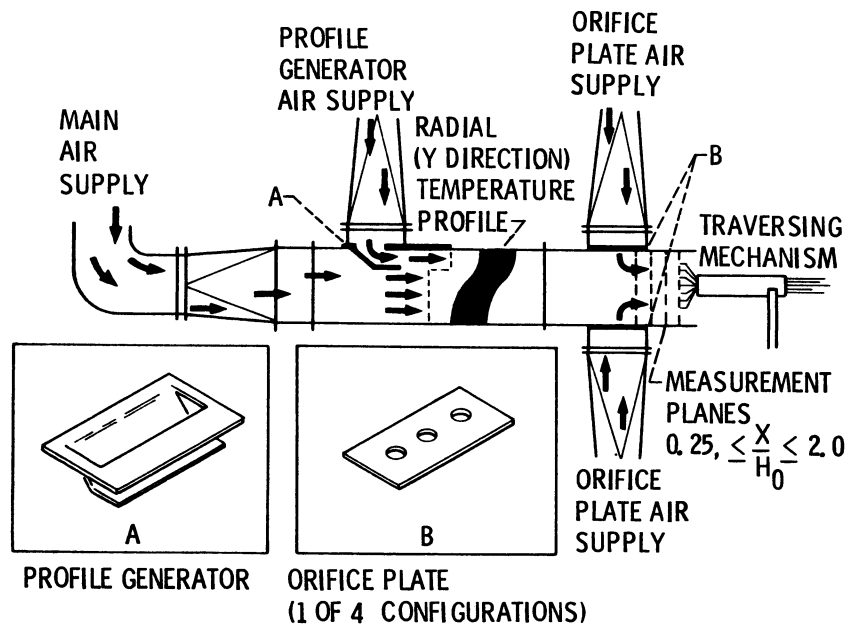


Figure 1. - Dilution jet mixing flow schematic.

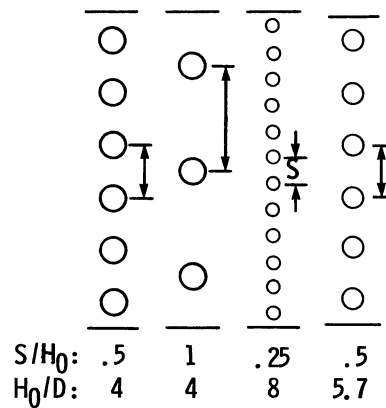


Figure 2. - Orifice configurations.

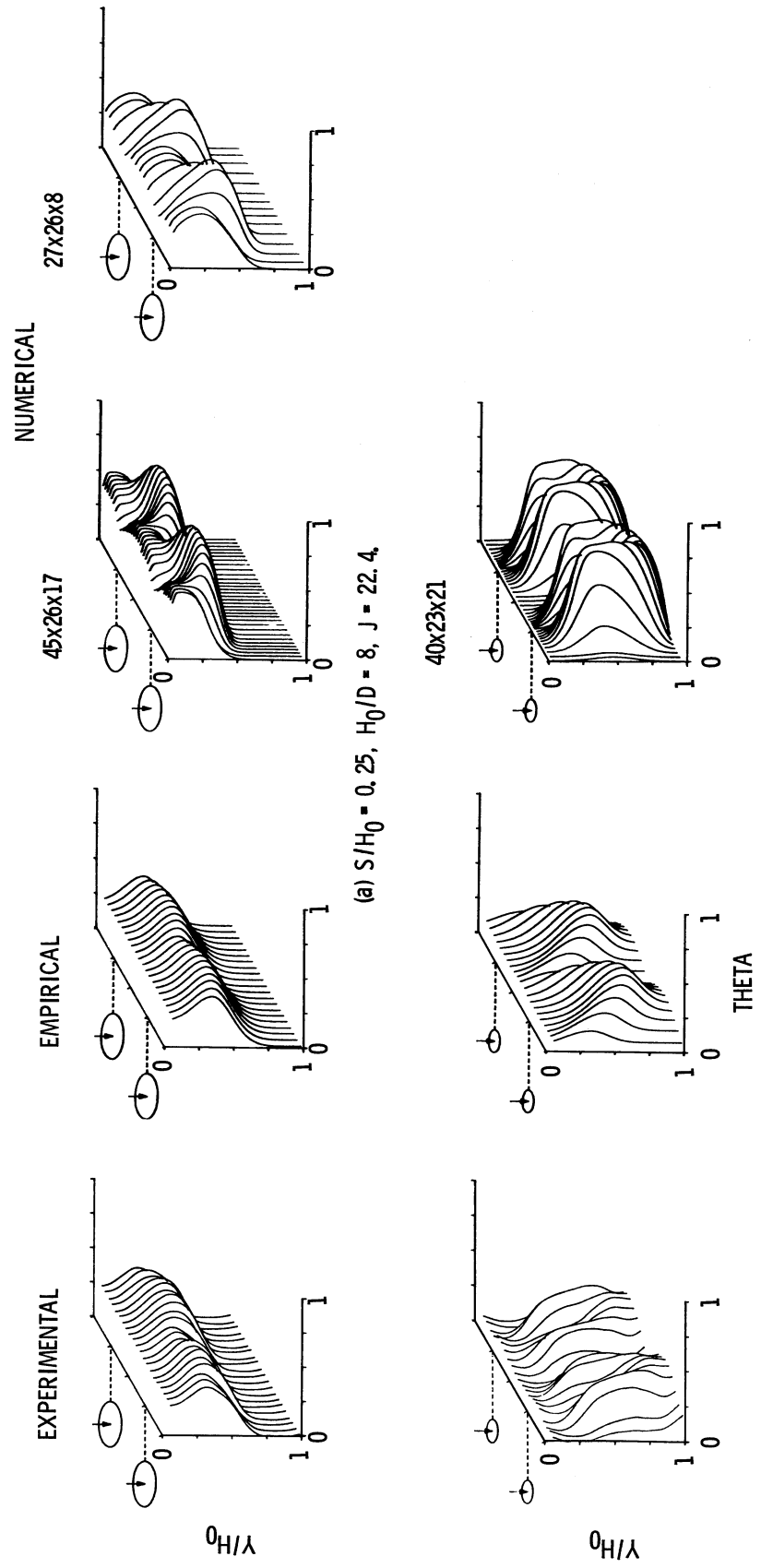
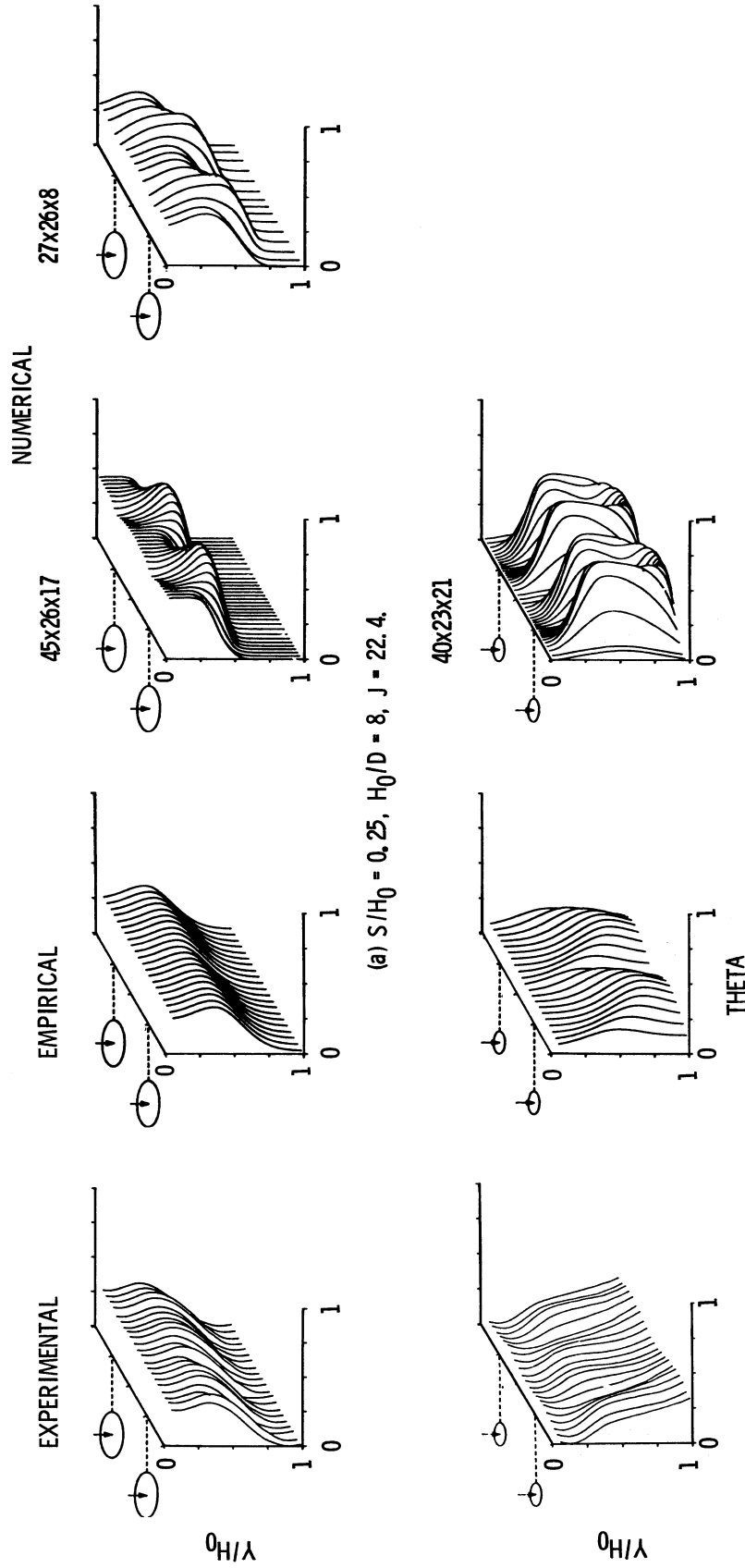


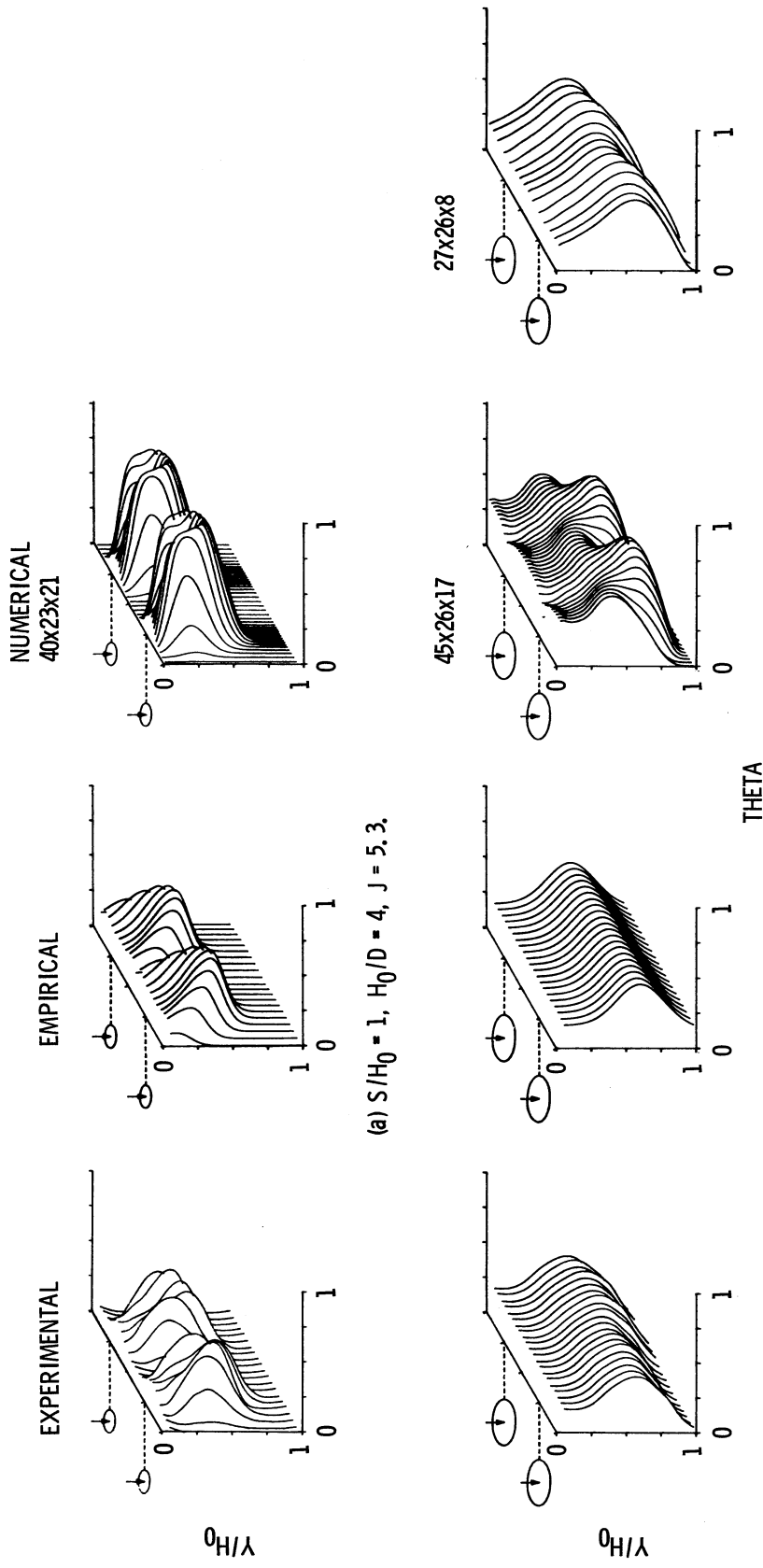
Figure 3. - Effect of varying orifice spacing at constant area; $A_j/A_m = 0.05$, $X/H_0 = 0.5$.



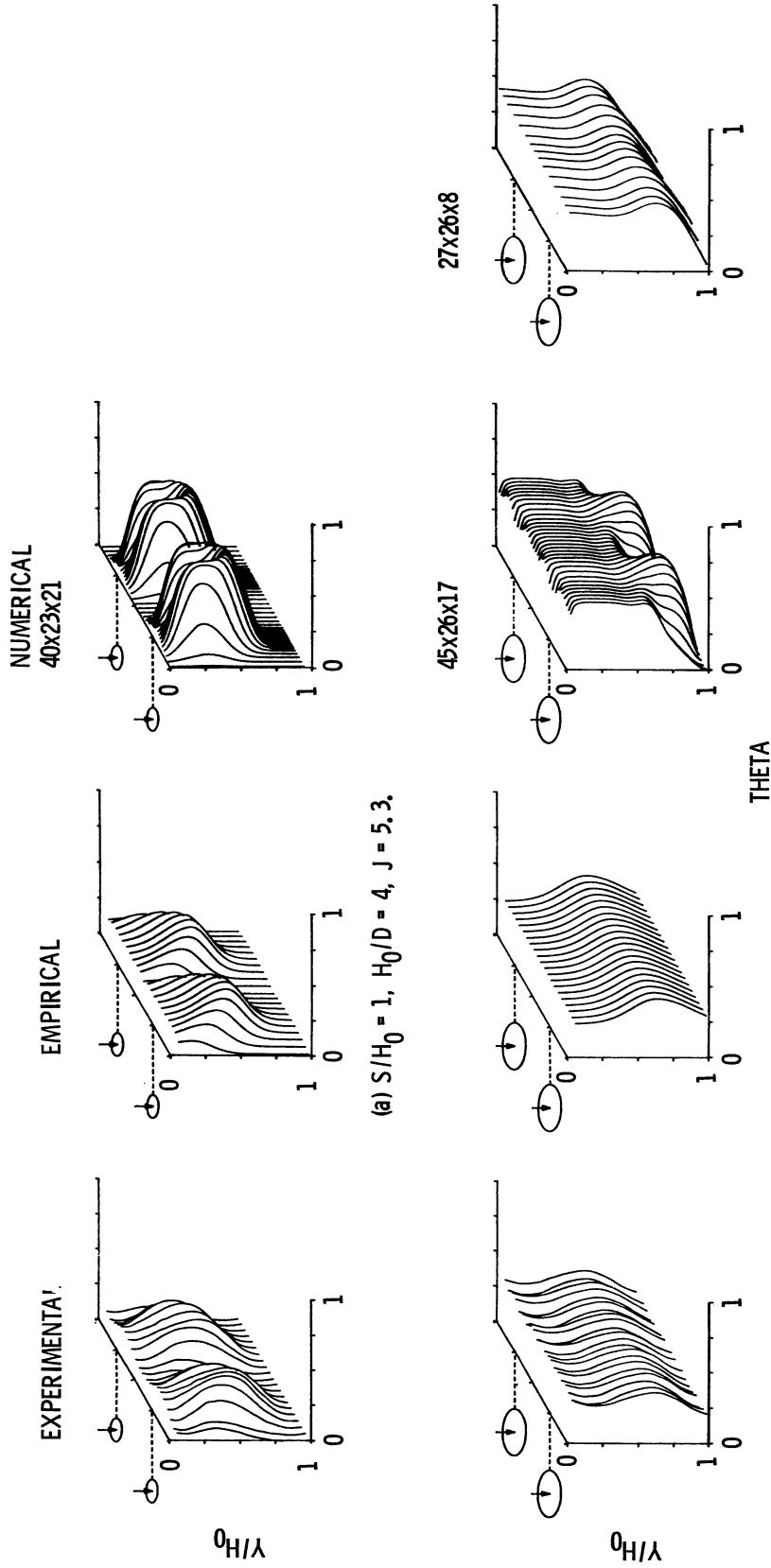
(a) $S/H_0 = 0.25$, $H_0/D = 8$, $J = 22.4$.

(b) $S/H_0 = 1$, $H_0/D = 4$, $J = 23.5$.

Figure 4. - Effect of varying orifice spacing at constant area; $A_j/A_m = 0.05$, $X/H_0 = 1$.



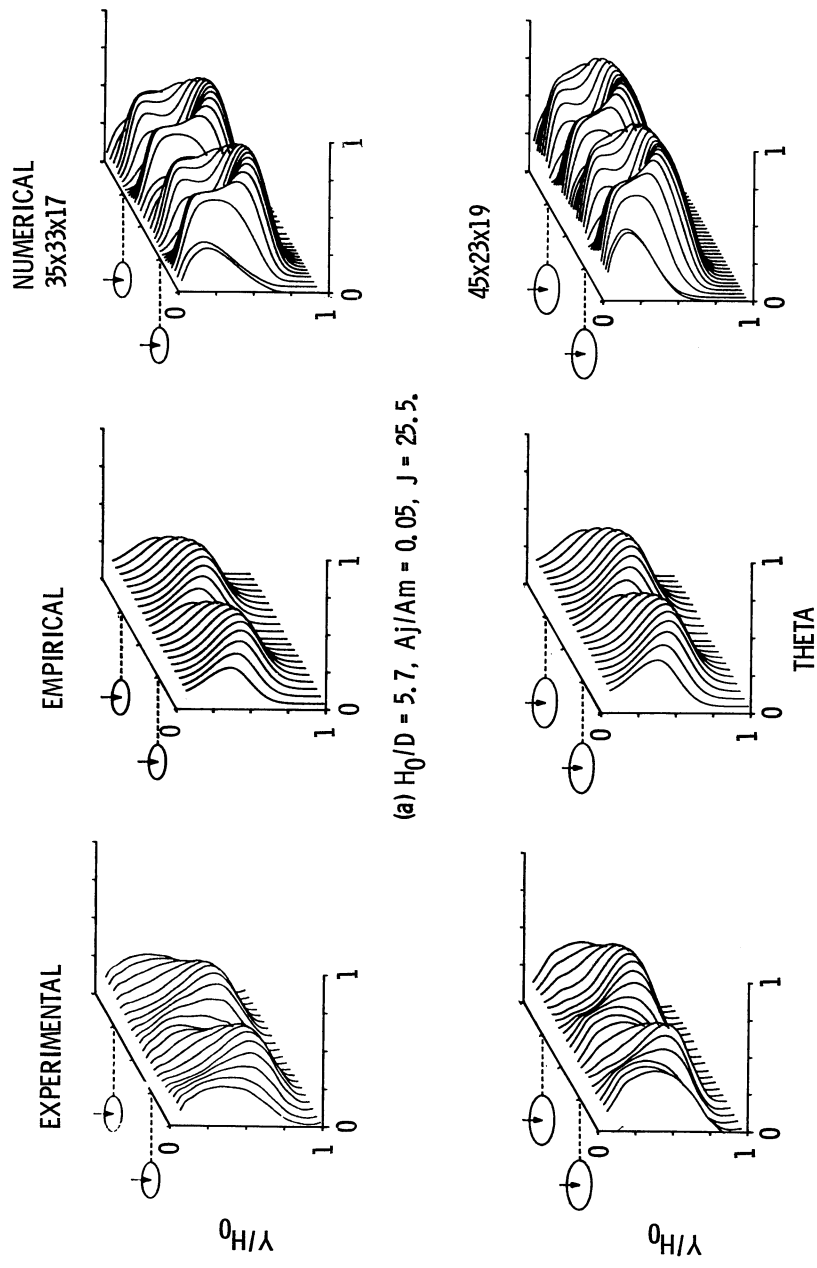
(a) $S/H_0 = 1$, $H_0/D = 4$, $J = 5.3$.
 (b) $S/H_0 = 0.25$, $H_0/D = 8$, $J = 92.7$.
 Figure 5. - Temperature distributions for coupled spacing and momentum flux ratio; $A_j/A_m = 0.05$, $X/H_0 = 0.5$.



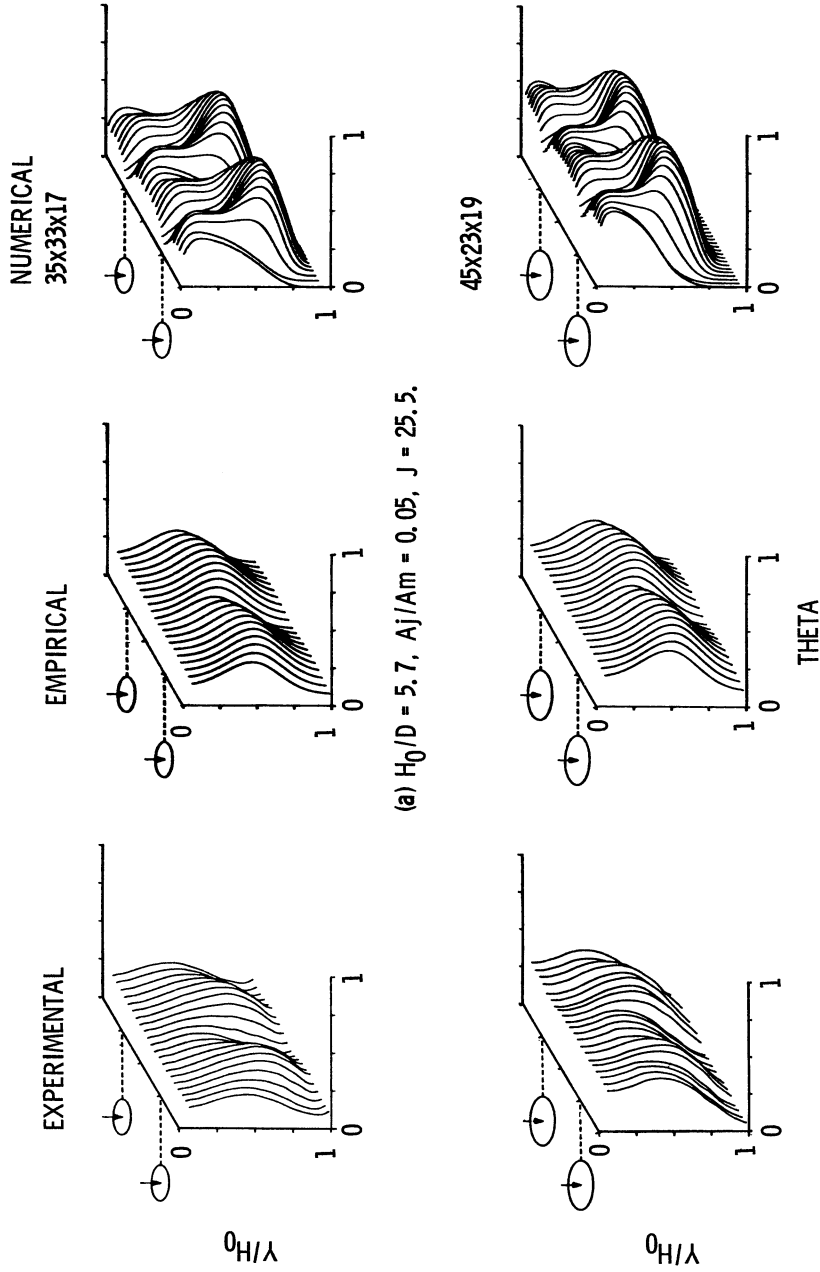
(a) $S/H_0 = 1$, $H_0/D = 4$, $J = 5.3$.

(b) $S/H_0 = 0.25$, $H_0/D = 8$, $J = 92.7$.

Figure 6. - Temperature distributions for coupled spacing and momentum flux ratio, $A_j/A_m = 0.05$, $X/H_0 = 1$.



(a) $H_0/D = 5.7$, $A_j/A_m = 0.05$, $J = 25.5$.
 (b) $H_0/D = 4$, $A_j/A_m = 0.10$, $J = 18.6$.
 Figure 7. - Effect of varying orifice diameter at constant spacing; $S/H_0 = 0.5$, $X/H_0 = 0.5$.



(a) $H_0/D = 5.7$, $A_j/A_m = 0.05$, $J = 25.5$.
 (b) $H_0/D = 4$, $A_j/A_m = 0.10$, $J = 18.6$.
 Figure 8. - Effect of varying orifice diameter at constant spacing; $S/H_0 = 0.5$, $X/H_0 = 1$.

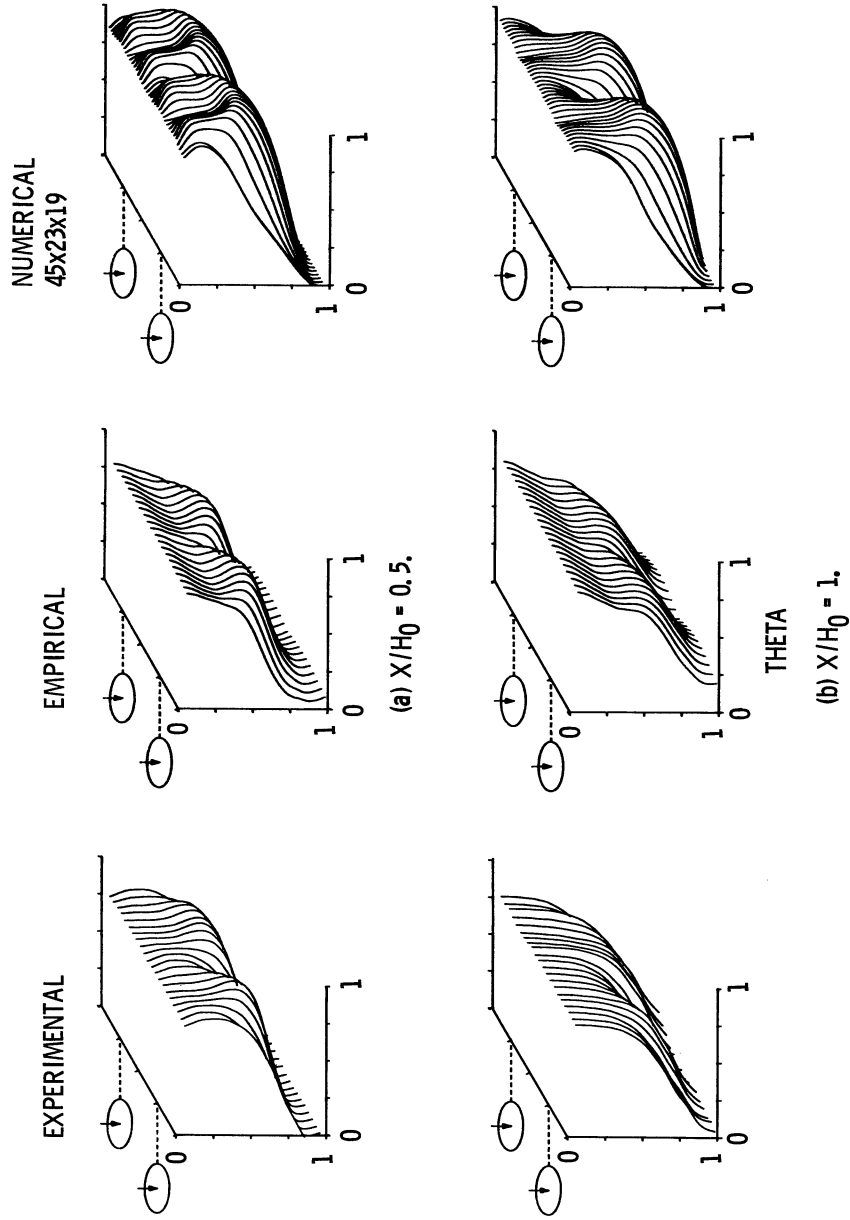


Figure 9. - Temperature mainstream; top cold, $S/H_0 = 0.5$, $H_0/D = 4$, $A_j/A_m = 0.10$, $J = 31.3$.

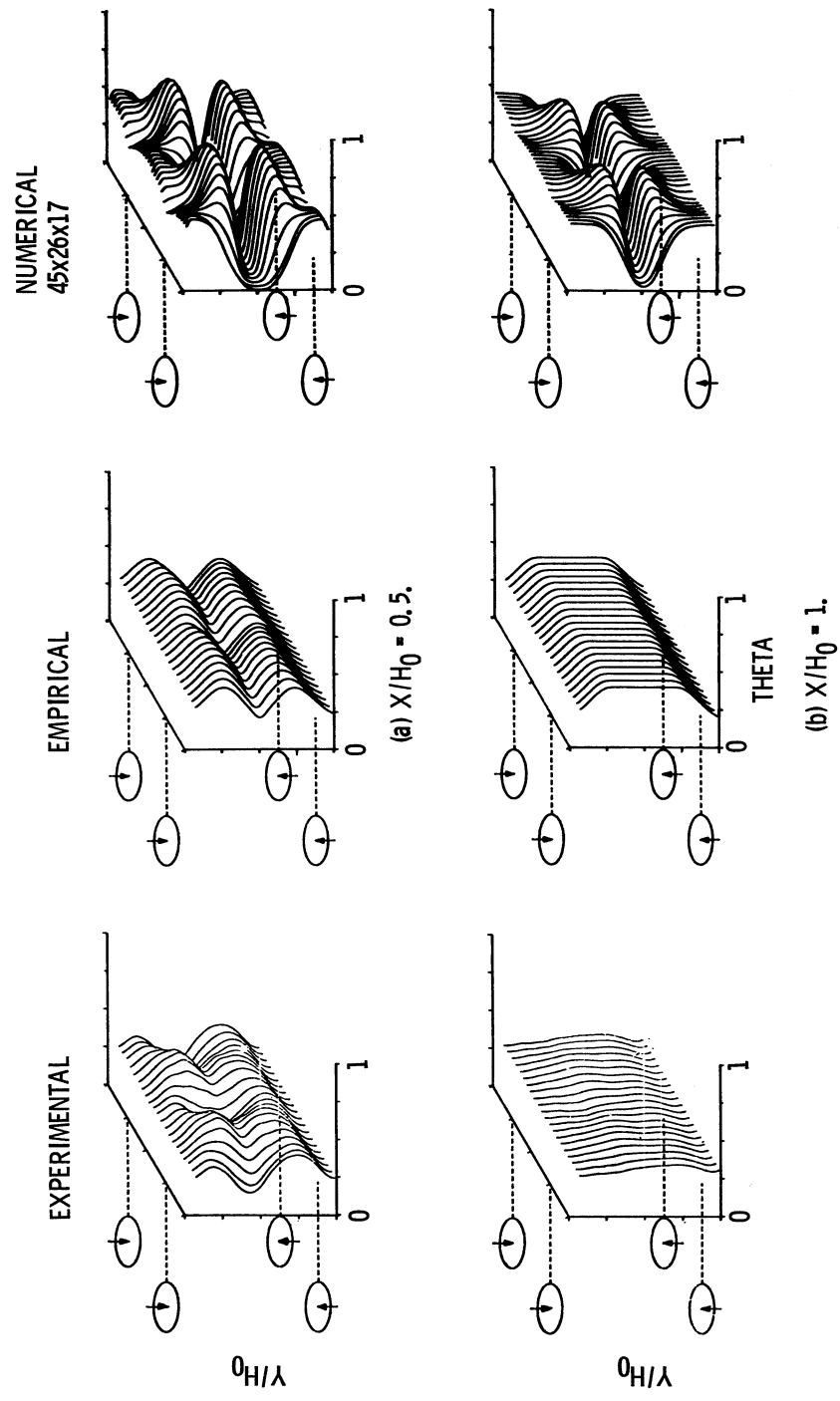


Figure 10. - Temperature distributions for opposed rows of in-line jets; $S/H_0 = 0.25$, $H_0/D = 8$, $A_j/A_m = 0.10$, $J = 25.0$.

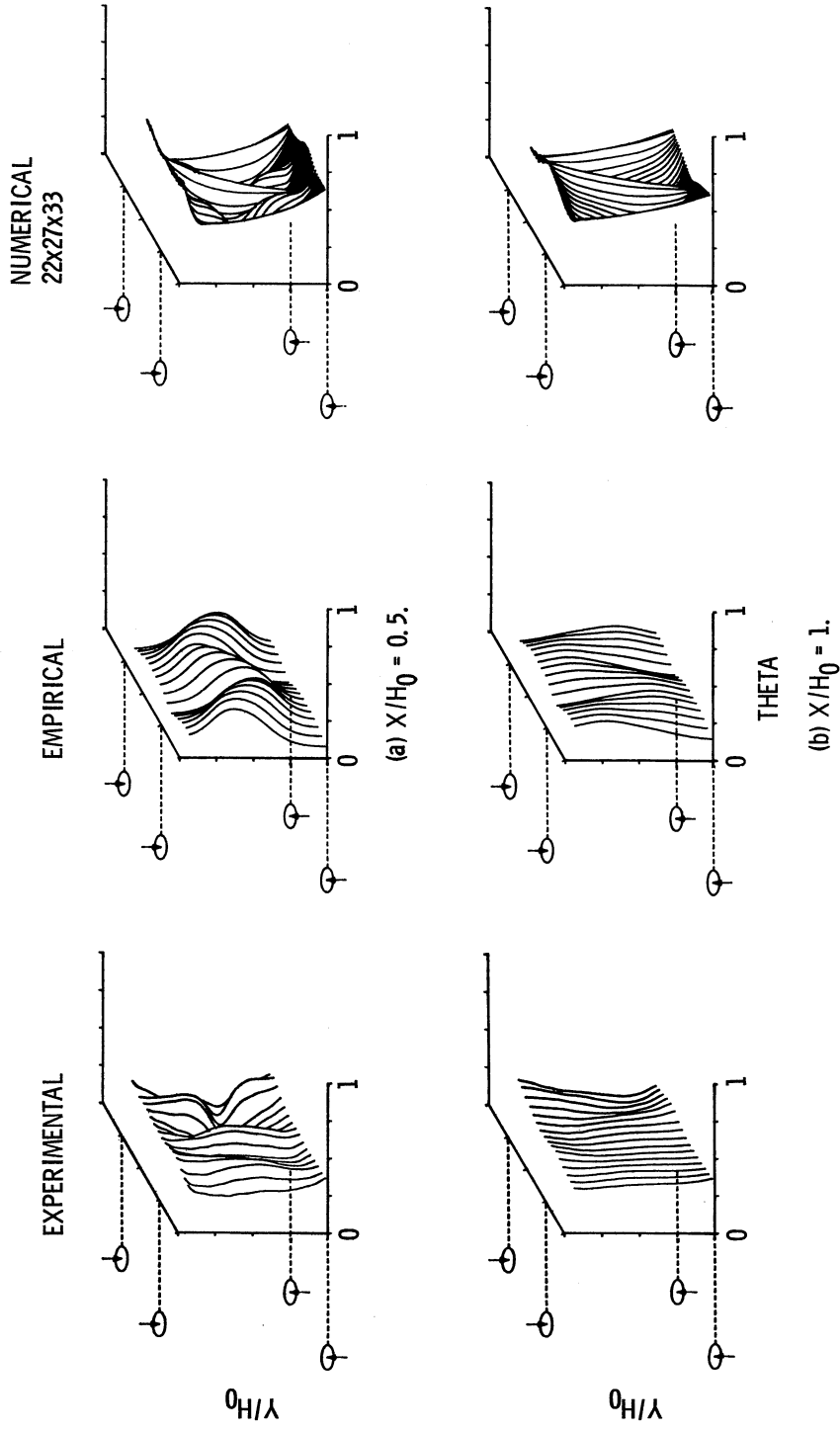


Figure 11. - Temperature distributions for opposed rows of staggered jets; $S/H_0 = 1$, $H_0/D = 4$, $A_j/Am = 0.10$, $J = 27.6$.

REPORT DOCUMENTATION PAGE

Form Approved
OMB No. 0704-0188

Public reporting burden for this collection of information is estimated to average 1 hour per response, including the time for reviewing instructions, searching existing data sources, gathering and maintaining the data needed, and completing and reviewing the collection of information. Send comments regarding this burden estimate or any other aspect of this collection of information, including suggestions for reducing this burden, to Washington Headquarters Services, Directorate for Information Operations and Reports, 1215 Jefferson Davis Highway, Suite 1204, Arlington, VA 22202-4302, and to the Office of Management and Budget, Paperwork Reduction Project (0704-0188), Washington, DC 20503.

| | | | |
|-------------------------------------------------------------------------------------------------------------------------------------------------------------------------------------------------------------------------------------------------------------------------------------------------------------------------------------------------------------------------------------------------------------------------------------------------------------------------------------------------------------------------------------------------------------------------------------------------------------------------------------------------------------------------------------|-----------------------------------------------------------------|--------------------------------------------------------------------------------------------|-----------------------------------|
| 1. AGENCY USE ONLY (<i>Leave blank</i>) | 2. REPORT DATE June 1984 | 3. REPORT TYPE AND DATES COVERED Technical Memorandum | |
| 4. TITLE AND SUBTITLE On Modeling Dilution Jet Flowfields | | 5. FUNDING NUMBERS WU-533-04-1A-00 | |
| 6. AUTHOR(S) J.D. Holdeman and R. Srinivasan | | | |
| 7. PERFORMING ORGANIZATION NAME(S) AND ADDRESS(ES) National Aeronautics and Space Administration Lewis Research Center Cleveland, Ohio 44135-3191 | | 8. PERFORMING ORGANIZATION REPORT NUMBER E-2168 | |
| 9. SPONSORING/MONITORING AGENCY NAME(S) AND ADDRESS(ES) National Aeronautics and Space Administration Washington, DC 20546-0001 | | 10. SPONSORING/MONITORING AGENCY REPORT NUMBER NASA TM-83708 AIAA-84-1379 | |
| 11. SUPPLEMENTARY NOTES J.D. Holdeman, Lewis Research Center; R. Srinivasan, The Garrett Turbine Engine Company, P.O. Box 5217, Phoenix, Arizona 85010. Prepared for the Twentieth Joint Propulsion Conference cosponsored by the AIAA, SAE, and ASME, Cincinnati, Ohio, June 11-13, 1984. | | | |
| 12a. DISTRIBUTION/AVAILABILITY STATEMENT Unclassified - Unlimited Subject Category 07 This publication is available from the NASA Center for Aerospace Information, (301) 621-0390. | | 12b. DISTRIBUTION CODE | |
| 13. ABSTRACT (<i>Maximum 200 words</i>) This paper compares temperature field measurements from selected experiments on a single row, and opposed rows, of jets injected into a ducted crossflow with profiles calculated using an empirical model based on assumed vertical profile similarity and superposition, and distributions calculated with a 3-D elliptic code using a standard K-E turbulence model. The empirical model predictions are very good within the range of the generating experiments, and the numerical model results, although exhibiting too little mixing, correctly describe the effects of the principal flow and geometric variables. | | | |
| 14. SUBJECT TERMS Dilution; Jet; Mixing | | | 15. NUMBER OF PAGES 19 |
| | | | 16. PRICE CODE |
| 17. SECURITY CLASSIFICATION OF REPORT Unclassified | 18. SECURITY CLASSIFICATION OF THIS PAGE Unclassified | 19. SECURITY CLASSIFICATION OF ABSTRACT Unclassified | 20. LIMITATION OF ABSTRACT |